On the stability of residual-free bubbles for convection-diffusion problems and their approximation by a two-level finite element method

L.P. Franca, A. Neslitürk

Department of Mathematics
University of Colorado at Denver
P.O. Box 173364, Campus Box 170
Denver, CO 80217-3364, USA

M. Stynes

Department of Mathematics
University College
Cork, IRELAND

Abstract

We consider the Galerkin finite element method for partial diffferential equations in two dimensions, where the finite-dimensional space used consists of piecewise (isoparametric) polynomials enriched with bubble functions. Writing L for the differential operator, we show that for elliptic convection-diffusion problems, the component of the bubble enrichment that stabilizes the method is equivalent to a Petrov-Galerkin method with an L-spline (exponentially fitted) trial space and piecewise polynomial test space; the remaining component of the bubble influences the accuracy of the method. A stability inequality recently obtained by Brezzi, Franca and Russo for a limiting case of bubbles applied to convection-diffusion problems is shown to be slightly weaker than the standard stability inequality that is obtained for the SDFEM/SUPG method, thereby demonstrating that the bubble approach is in general slightly less stable than the streamline diffusion method. When the trial functions are piecewise linear, we show that residual-free bubbles are as stable as SDFEM/SUPG, and we extend this stability inequality to include positive mesh-Peclet numbers in the convection-dominated regime. Approximate computations of the residual-free bubbles are performed using a two-level finite element method.

1 Introduction

The Galerkin finite element method, with standard piecewise polynomials enriched by *bubble functions*, has been a fruitful source of discretizations for partial differential equations whose solution by standard methods is fraught with difficulties. For examples of this technique, see [3, 5, 10, 11, 12, 1, 2, 6]. In the present paper we shall concentrate on the variant of this method known as *residual-free bubbles* (RFB) [3, 5, 10, 11, 12, 14], but we also indicate how other bubble variants fit into the same analytical framework.

We consider partial differential equations in a two-dimensional domain Ω that is partitioned into a mesh of elements K (e.g., triangles or quadrilaterals). On each K, our computed solution is the sum of a piecewise (isoparametric) polynomial and a bubble function that vanishes on the boundary of K, ∂K. In the RFB approach, this bubble function is chosen so that the computed solution satisfies the differential equation in the interior of each K. While this yields a stable and satisfactory numerical method for convection-diffusion problems, the mechanism by which the RFB method achieved stability was until recently an open problem; then, in [4] Brezzi et al. proved a new coercivity/stability inequality for a limiting case of this method. Their stability result is couched in an interesting and unusual norm that has not previously been used in the convection-diffusion research literature. We shall extend their argument to the case of large mesh-Peclet number with piecewise linear polynomials. We show that in general this norm is slightly weaker than the norm that appears in typical analyses of the streamline diffusion (SDFEM/SUPG) method [7, 16]. It will also be shown that, reformulating the RFB method in a Petrov-Galerkin framework with L-spline trial functions and piecewise linear test functions, the stability of the RFB method is due to this particular combination of trials and tests. This reformulation reveals that part of the bubble function gives the method its stability, and the remainder of that function controls the consistency/accuracy of the method. This insight is also applicable to other (non-RFB) bubble functions.

We then proceed to approximate the computations of the residual-free bubbles by a two-level finite element method [8]. We partition our mesh into submeshes, and a suitable numerical method is used to approximate the PDE's governing the residual-free-bubbles basis functions. Herein we use the Galerkin-least squares (GLS) method [7, 15] to approximate these equations in a coarse mesh for each element. Numerical results are presented for this two-level method and contrasted with computations with the usual GLS method for the original mesh.

The structure of the paper is as follows. In the next Section we review the RFB method. Then in Section 3 we apply it to the convection-diffusion equation. Therein we split the RFB method in a way that shows its intimate connection with L-spline Petrov-Galerkin methods (here L is the convection-diffusion operator) and then analyse its stability. We also prove the relationship described above between the norm of [4] and the streamline diffusion norm. Then the approximation of the RFB's basis functions are described using a two-level finite element method in Section 4 and numerical results are presented in Section 5.

2 The Residual-Free Bubble (RFB) Method

Consider the boundary-value problem

$$\begin{cases} Lu = f & \text{in } \Omega\,, \\ u = 0 & \text{on } \partial\Omega\,, \end{cases} \tag{1}$$

where Ω is a domain in $\mathbb{R}^2$ with boundary $\partial\Omega$, L is a linear differential operator, u is the unknown scalar function and f is a given source function. We assume that L is such that this problem is well posed.

To specify a Galerkin finite element method for (1), we begin by partitioning Ω into elements K (triangles, quadrilaterals, etc.) in the standard way (e.g., no overlapping, no vertex on the edge of a neighbouring element, etc.), then we choose a finite-dimensional space V_h which is related to the choice of partition and which satisfies $V_h \subset V$, where V is the space of functions in which we seek a solution of the continuous problem. Here $h = \max_K\{\mathrm{diam}(K)\}$ is the mesh diameter. Then the Galerkin method is: find $u_h \in V_h$ such that

$$a(u_h, v_h) = (f, v_h) \quad \forall v_h \in V_h\,, \tag{2}$$

where $a(\cdot,\cdot)$ is a suitable weak form of (1) and $(\cdot,\cdot)$ is the L_2 inner product on Ω.

For Galerkin methods that use bubbles, each $v_h \in V_h$ is the sum of a standard piecewise (isoparametric) polynomial and a bubble function that we precisely define later. Thus we write

$$v_h = v_1 + v_b, \tag{3}$$

where v_1 is the polynomial component of v_h (the subscript "1" is used as we are primarily interested in linear and bilinear polynomials), and v_b is its bubble component. Similarly we write

$$u_h = u_1 + u_b\,, \tag{4}$$

where we recall that u_h is the solution of (2).

All forms of bubble functions [1, 2, 3, 5, 6, 10, 11, 12] are required to vanish on the boundary ∂K of each K (except for "macro-bubbles" that vanish on the boundary of a patch of elements [9] and L-splines that vanish on vertices [20]). For the particular case of the residual-free bubble, we define the bubble component v_b of each v_h by also requiring v_h to satisfy the original differential equation on the interior of each K, i.e,

$$Lv_h = L(v_1 + v_b) = f \quad \text{in } K \text{ for all } K.$$

In particular this implies that for each K we have

$$Lu_b = -Lu_1 + f \qquad \text{in } K. \tag{5}$$

For general (possibly residual-free) bubbles, the vanishing of the bubble functions on each ∂K allows us to use the classical *static condensation* procedure: in (2) take $v_h = v_b$ on K and $v_h = 0$ elsewhere to obtain

$$a(u_1 + u_b, v_b)_K = (f, v_b)_K \tag{6}$$

where the subscript K indicates that integration is restricted to the element K. On each element, this equation provides us with the bubble part u_b of the solution as a function

of the piecewise polynomial part u_1. (Our choice above of residual-free bubbles ensures that equation (6) is satisfied automatically; we presented the general static condensation technique here to allow our later arguments to encompass other types of bubbles.)

Then the numerical method that we implement is got by setting $v_h = v_1$ in (2), which gives

$$a(u_1, v_1) + a(u_b, v_1) = (f, v_1) \quad \text{for all } v_1 \in V_{h1}, \tag{7}$$

where V_{h1} is our space of piecewise polynomials and u_b is given in terms of u_1 by (6). Thus our elimination of the bubbles may be viewed as a modification of the variational formulation of the standard piecewise polynomial Galerkin method by the addition of $a(u_b, v_1)$ to the left-hand side.

3 Convection-Diffusion Problem

We now consider the case where L is a convection-diffusion operator. Convection-diffusion problems have many practical applications and their numerical solution has been extensively studied; see [19] for a description and bibliography of a large number of numerical methods applicable to such problems.

Thus we set

$$L = -\kappa\triangle + \boldsymbol{a} \cdot \nabla\,, \tag{8}$$

where κ is a small positive constant and $\boldsymbol{a} \neq \boldsymbol{0}$ is the velocity field. We assume for simplicity that $\boldsymbol{a}$ is constant on Ω, where $|\cdot|$ is the Euclidean norm in $\mathbb{R}^2$, but almost all of our analysis remains valid if $\boldsymbol{a}$ is a piecewise constant approximation (on the partition of Ω) of a smooth velocity field. The associated bilinear form is

$$a(v, w) := \sum_K \big(\kappa(\nabla v, \nabla w)_K + (\boldsymbol{a} \cdot \nabla v, w)_K\big), \tag{9}$$

where we integrate over the interior of each K separately in order to avoid any possible difficulties of interpretation at element boundaries.

In [4], Brezzi et al. showed that this bilinear form was coercive in the limit as $\kappa \to 0$, using some reasonable simplifying assumptions about the form of the bubble function on each K. We shall prove a similar result here for the case when V_{h1} is the space of piecewise linears, and the mesh-Peclet number is large.

Let $v_h \in V_h$ be arbitrary. Then $v_h = v_1 + v_b$. We decompose v_b further as $v_b = v_b^0 + v_b^f$, where v_b^0 is defined on each K by

$$\begin{cases} Lv_b^0 = -Lv_1 & \text{in } K, \\ v_b^0 = 0 & \text{on } \partial K, \end{cases} \tag{10}$$

Now set $\tilde{v}_h = v_1 + v_b^0$. That is, $\tilde{v}_h$ is defined by

$$\begin{cases} L\tilde{v}_h = 0 & \text{in } K, \\ \tilde{v}_h = v_h = v_1 & \text{on } \partial K, \end{cases} \tag{11}$$

This definition states that $\tilde{v}_h$ is an *L-spline* (or *exponentially fitted* function) on the interior of each K. Similar functions have been used by many authors as trial functions in finite element methods for convection-diffusion problems; see for example [13, 17, 19, 20]. Nevertheless the analysis of such methods is not well developed.

From (7), the numerical method can be written as

$$a(\tilde{u}_h, v_1) = -a(u_b^f, v_1) + (f, v_1) \quad \text{for all } v_1 \in V_{h1}, \tag{12}$$

where, analogously to the definition of $\tilde{v}_h$, we decompose u_b as $u_b = u_b^0 + u_b^f$, then set $\tilde{u}_h = u_1 + u_b^0$.

Let $\tilde{V}_h = \{\tilde{v}_h : v_h \in V_h\}$. We shall prove that the bilinear form $a(\cdot,\cdot)$ is coercive over $\tilde{V}_h \times V_{h1}$, under the assumptions that V_{h1} is the space of piecewise linears on triangles K, that the triangulation is regular, and this regularity is uniform as $h \to 0$. (We shall also make mild assumptions later on the orientation of the mesh and the relationship between κ and $\min_K h_K$, where h_K is the diameter of K.)

Thus, let $v_h \in V_h$ be arbitrary, and consider $a(\tilde{v}_h, v_1)$. We write $||\cdot||_{0,D}$ for the $L^2(D)$ norm on any domain D, and $|\cdot|_{1,K}$ for the standard $H^1(K)$ seminorm. From (9),

$$\begin{aligned} a(\tilde{v}_h, v_1) &= \sum_K \big(\kappa(\nabla\tilde{v}_h, \nabla v_1)_K + (\boldsymbol{a}\cdot\nabla\tilde{v}_h, v_1)_K\big) \\ &= \sum_K \big(\kappa|v_1|_{1,K}^2 + \kappa(\nabla v_b^0, \nabla v_1)_K + (\boldsymbol{a}\cdot\nabla v_1, v_1)_K + (\boldsymbol{a}\cdot\nabla v_b^0, v_1)_K\big) \\ &= \sum_K \big(\kappa|v_1|_{1,K}^2 + (\boldsymbol{a}\cdot\nabla v_1, v_1)_K - (v_b^0, \boldsymbol{a}\cdot\nabla v_1)_K\big), \end{aligned} \tag{13}$$

where we integrated by parts twice and used the facts that $v_b^0 = 0$ on each ∂K, $\boldsymbol{a}$ is constant and $\Delta v_1 = 0$ on each K since v_1 is linear.

For each triangle K, let $\partial K^- = \{\boldsymbol{x} \in \partial K : \boldsymbol{a}\cdot\boldsymbol{n}(\boldsymbol{x}) < 0\}$ be its inflow boundary and $\partial K^+ = \{\boldsymbol{x} \in \partial K : \boldsymbol{a}\cdot\boldsymbol{n}(\boldsymbol{x}) > 0\}$ its outflow boundary, where $\boldsymbol{n}$ is the outward-pointing unit normal to ∂K. Assume that $\boldsymbol{a}\cdot\boldsymbol{n}(\boldsymbol{x})$ is bounded away from zero; then, excluding vertices, for each K we have $\partial K = \partial K^- \cup \partial K^+$. (A similar condition appears in analyses of the discontinuous Galerkin method, see [19].)

Let $\hat{v}_b^0$ be the reduced solution of (10), i.e., for each K,

$$\begin{cases} \boldsymbol{a}\cdot\nabla\hat{v}_b^0 = -\boldsymbol{a}\cdot\nabla v_1 & \text{in } K, \\ \hat{v}_b^0 = 0 & \text{on } \partial K^-. \end{cases} \tag{14}$$

Let (x^-, x^+) be a generic line segment that lies in a single K with $x^- \in \partial K^-$ and $x^+ \in \partial K^+$. Clearly

$$\hat{v}_b^0(x) = v_1(x^-) - v_1(x) \quad \text{for } x \in (x^-, x^+). \tag{15}$$

Hence, recalling (13), we have

$$\begin{aligned} a(\tilde{v}_h, v_1) = \sum_K \big(&\kappa|v_1|_{1,K}^2 + (\boldsymbol{a}\cdot\nabla v_1, v_1)_K + (v_1, \boldsymbol{a}\cdot\nabla v_1)_K \\ &-(v_1(x^-), \boldsymbol{a}\cdot\nabla v_1)_K + (\hat{v}_b^0 - v_b^0, \boldsymbol{a}\cdot\nabla v_1)_K\big), \end{aligned} \tag{16}$$

Now Brezzi et al. [4] show that

$$\sum_K \big((v_1, \boldsymbol{a}\cdot\nabla v_1)_K - (v_1(x^-), \boldsymbol{a}\cdot\nabla v_1)_K\big) = \sum_K \frac{1}{2|\boldsymbol{a}|^2}\int_{x^+\in\partial K^+}\left(\int_{x^-}^{x^+}\boldsymbol{a}\cdot\nabla v_1\,ds\right)^2 \boldsymbol{a}\cdot\boldsymbol{n}\,d\Gamma.$$

Using this identity and noting that $\boldsymbol{a}$ constant implies that $(\boldsymbol{a}\cdot\nabla v_1, v_1) = 0$ (as $v_1 = 0$ on $\partial\Omega$), we see that (16) simplifies to

$$a(\tilde{v}_h, v_1) = \sum_K \left(\kappa|v_1|^2_{1,K} + \frac{1}{2|\boldsymbol{a}|^2}\int_{x^+\in\partial K^+}\left(\int_{x^-}^{x^+}\boldsymbol{a}\cdot\nabla v_1\,ds\right)^2 \boldsymbol{a}\cdot\boldsymbol{n}\,d\Gamma\right) + \sum_K(\hat{v}_b^0 - v_b^0, \boldsymbol{a}\cdot\nabla v_1)_K. \tag{17}$$

To complete the coercivity analysis, we shall show that the third term in this sum is dominated by the second term. The expression appearing in this second term is rather unusual; in the next two Lemmas, we show that in general it is weaker than the seminorm that appears in standard analyses of the streamline diffusion finite element method (SDFEM/SUPG), but on the piecewise linear space V_{h1} it is equivalent to this seminorm.

Lemma 1 *Let w be any function that is defined and differentiable on Ω. Then for each triangle K we have*

$$\int_{x^+\in\partial K^+}\left(\int_{x^-}^{x^+}\boldsymbol{a}\cdot\nabla v_1\,ds\right)^2 \boldsymbol{a}\cdot\boldsymbol{n}\,d\Gamma \le h_K|\boldsymbol{a}|\int_K(\boldsymbol{a}\cdot\nabla v_1)^2\,ds,$$

where h_K is the diameter of K.

Proof: By the Cauchy-Schwarz inequality,

$$\begin{aligned}\int_{x^+\in\partial K^+}\left(\int_{x^-}^{x^+}\boldsymbol{a}\cdot\nabla v_1\,ds\right)^2 \boldsymbol{a}\cdot\boldsymbol{n}\,d\Gamma &\le \int_{x^+\in\partial K^+}\left(\int_{x^-}^{x^+}1^2\,ds\right)\left(\int_{x^-}^{x^+}(\boldsymbol{a}\cdot\nabla v_1)^2\,ds\right)\boldsymbol{a}\cdot\boldsymbol{n}\,d\Gamma\\ &\le h_K\int_{x^+\in\partial K^+}\int_{x^-}^{x^+}(\boldsymbol{a}\cdot\nabla v_1)^2\,ds\,\boldsymbol{a}\cdot\boldsymbol{n}\,d\Gamma\\ &\le h_K|\boldsymbol{a}|\int_K(\boldsymbol{a}\cdot\nabla v_1)^2\,dK.\end{aligned}$$

■

Lemma 2 *Let v_1 be any piecewise linear function that is defined on the triangulation of Ω, and assume that this triangulation is regular. Then for each triangle K there exists a positive constant C_2, which depends only on the regularity of triangulation, such that*

$$C_2\frac{h_K}{2|\boldsymbol{a}|}\int_K(\boldsymbol{a}\cdot\nabla v_1)^2\,ds \le \frac{1}{2|\boldsymbol{a}|^2}\int_{x^+\in\partial K^+}\left(\int_{x^-}^{x^+}\boldsymbol{a}\cdot\nabla v_1\,ds\right)^2 \boldsymbol{a}\cdot\boldsymbol{n}\,d\Gamma.$$

Proof: Now $\boldsymbol{a}\cdot\nabla v_1$ is constant on each K, so

$$\begin{aligned}\frac{1}{2|\boldsymbol{a}|^2}\int_{x^+\in\partial K^+}\left(\int_{x^-}^{x^+}\boldsymbol{a}\cdot\nabla v_1\,ds\right)^2\boldsymbol{a}\cdot\boldsymbol{n}\,d\Gamma &= \frac{1}{2|\boldsymbol{a}|^2}\int_{x^+\in\partial K^+}(x^+-x^-)^2(\boldsymbol{a}\cdot\nabla v_1)_K^2\,\boldsymbol{a}\cdot\boldsymbol{n}\,d\Gamma\\ &\geq C_1\frac{h_K^3}{2|\boldsymbol{a}|}(\boldsymbol{a}\cdot\nabla v_1)_K^2\\ &\geq C_2\frac{h_K}{2|\boldsymbol{a}|}\int_K(\boldsymbol{a}\cdot\nabla v_1)^2\,dK\end{aligned}$$

for some constants C_1 and C_2, since $\boldsymbol{a}\cdot\boldsymbol{n}$ is bounded away from zero and the triangulation is regular. ■

We now return to the main thread of our analysis. On each K, the formulas (10) and (15) imply that

$$L(\hat{v}_b^0-v_b^0)=-\kappa\Delta\hat{v}_b^0$$

and

$$\begin{cases}\hat{v}_b^0-v_b^0=0 & \text{on } \partial K^-,\\ (\hat{v}_b^0-v_b^0)(x^+)=v_1(x^-)-v_1(x^+) & \text{for each } x^+\in\partial K.\end{cases}$$

Note here that

$$v_1(x^-)-v_1(x^+)=\frac{-1}{|\boldsymbol{a}|}\int_{x^-}^{x^+}\boldsymbol{a}\cdot\nabla v_1\,ds. \tag{18}$$

We need to bound $||\hat{v}_b^0-v_b^0||_{0,K}$ in order to handle the last term in (17). For this we have the following Lemma (where for convenience we set $z=\hat{v}_b^0-v_b^0$):

Lemma 3 *Let K be a fixed triangle in our triangulation. Suppose that z is defined on K by*

$$\begin{cases}Lz=-\kappa\Delta\hat{v}_b^0 & \text{in } K,\\ z=0 & \text{on } \partial K^-,\\ z=\phi & \text{on } \partial K^+,\end{cases} \tag{19}$$

where $\phi(x^+)=v_1(x^-)-v_1(x^+)$. Then there exists a fixed positive constant C_5, which is independent of κ, h_K and $|\boldsymbol{a}|$, such that

$$||z||_{0,K}\leq C_5\left(\frac{\kappa^{1/2}h_K^{1/2}}{|\boldsymbol{a}|^{3/2}}+\frac{\kappa}{|\boldsymbol{a}|^2}\right)||\boldsymbol{a}\cdot\nabla v_1||_{0,K}.$$

Proof: If ∂K^- is a single side of K, then $-\kappa\Delta\hat{v}_b^0=0$ on K, but in general this is not the case.

Define the function Φ on K by

$$\begin{cases}L\Phi=0 & \text{in } K,\\ \Phi=0 & \text{on } \partial K^-,\\ \Phi=\phi & \text{on } \partial K^+,\end{cases}$$

so that Φ is a smooth boundary-layer-like extension of ϕ over K. Now set $w = z - \Phi$. Then

$$\begin{cases} Lw = -\kappa\Delta\hat{v}_b^0 & \text{in } K, \\ w = 0 & \text{on } \partial K. \end{cases}$$

Unlike the rest of the paper, in this proof we shall for the most part use (x, y) as our coordinates in two dimensions. Since $\boldsymbol{a}$ is constant on K, without loss of generality we assume that $\boldsymbol{a} = a_1\vec{\imath}$ for some $a_1 > 0$, where $\vec{\imath}$ is the unit vector in the direction of the positive x axis.

Choose $(x^*, y^*) \in \partial K^+$ such that $x \le x^*$ for all $(x, y) \in K$. Multiply $Lw = -\kappa\Delta\hat{v}_b^0$ by $(x^* - x)w(x, y)$ and integrate over K; after an integration by parts we get

$$\begin{aligned} &\int_K (x^* - x)(-\kappa\Delta\hat{v}_b^0)(x, y)w(x, y)\,dx\,dy \\ &= \int_K \left[\kappa(x^* - x)|\nabla w(x, y)|^2 + \frac{a_1}{2}(x^* - x)\frac{\partial}{\partial x}w^2(x, y)\right]\,dx\,dy \\ &= \int_K \left[\kappa(x^* - x)|\nabla w(x, y)|^2 + (a_1/2)w^2(x, y)\right]\,dx\,dy, \end{aligned} \tag{20}$$

where we integrated by parts and used $w = 0$ on ∂K. Next, integrating the left-hand side of (20) by parts, we get

$$\begin{aligned} &\int_K \kappa\nabla\hat{v}_b^0(x, y) \cdot \nabla\big((x^* - x)w(x, y)\big)\,dx\,dy \\ &= \int_K \kappa\nabla\hat{v}_b^0(x, y) \cdot \big((x^* - x)\nabla w(x, y) - w(x, y)\vec{\imath}\big)\,dx\,dy \\ &\le \frac{1}{2}\int_K \left[\kappa(x^* - x)|\nabla w(x, y)|^2 + \frac{a_1}{2}w^2(x, y)\right]\,dx\,dy \\ &\qquad + \frac{1}{2}\int_K \left[\kappa(x^* - x)|\nabla\hat{v}_b^0(x, y)|^2 + \frac{\kappa^2}{a_1}|\nabla\hat{v}_b^0(x, y)|^2\right]\,dx\,dy. \end{aligned} \tag{21}$$

Combining (20) and (21), we infer that

$$\begin{aligned} \int_K w^2(x, y)\,dx\,dy &\le \frac{2}{a_1}\int_K \left(\kappa(x^* - x) + \frac{\kappa^2}{a_1}\right)|\nabla\hat{v}_b^0(x, y)|^2\,dx\,dy \\ &\le \frac{2}{a_1}\int_K \left(\kappa h_K + \frac{\kappa^2}{a_1}\right)|\nabla\hat{v}_b^0(x, y)|^2\,dx\,dy. \end{aligned}$$

Thus

$$||w||_{0,K} \le \sqrt{2}\left(\frac{\kappa^{1/2}h_K^{1/2}}{a_1^{1/2}} + \frac{\kappa}{a_1}\right)||\nabla\hat{v}_b^0||_{0,K}. \tag{22}$$

We must now bound $||\nabla\hat{v}_b^0||_{0,K}$. If ∂K^- consists only of a single edge of K, then $\hat{v}_b^0$ is linear on K and $\Delta\hat{v}_b^0 = 0$, so $w = 0$ and (23) holds true trivially. We therefore assume

that ∂K^- consists of two edges of K. Recall that the edges of each K are bounded away from being parallel to $\boldsymbol{a} = a_1\vec{\imath}$. This means that we can write the equations of the two edges in ∂K^- as $x = m_i y + k_i$ for $i = 1, 2$, where the m_i and k_i are constants that satisfy $|m_i| \le C_4$ for some fixed constant C_4.

Suppose that $v_1(x, y) = \alpha x + \beta y + \gamma$ on K. For $i = 1, 2$, if (x, y) lies in that part of K that is downwind of the side $x_i = m_i y + k_i$, then from (15) we have

$$\begin{aligned}\hat{v}_b^0(x, y) &= v_1(x^-, y) - v_1(x, y) \\ &= v_1(m_i y + k_i, y) - v_1(x, y) \\ &= \alpha(m_i y + k_i) + \beta y + \gamma - (\alpha x + \beta y + \gamma) \\ &= \alpha(m_i y + k_i - x),\end{aligned}$$

so

$$\left|\frac{\partial \hat{v}_b^0(x, y)}{\partial y}\right| = |\alpha m_i| \le C_4|\alpha| = C_4\left|\frac{\partial \hat{v}_b^0(x, y)}{\partial x}\right|.$$

(This inequality bounds the crosswind derivative of $\hat{v}_b^0$ in terms of the streamline derivative of this function.) Hence

$$\begin{aligned}||\nabla \hat{v}_b^0||_{0,K} &\le ||(\hat{v}_b^0)_x||_{0,K} + ||(\hat{v}_b^0)_y||_{0,K} \\ &\le ((1 + C_4)/a_1)||\boldsymbol{a} \cdot \nabla \hat{v}_b^0||_{0,K} \\ &= ((1 + C_4)/a_1)||\boldsymbol{a} \cdot \nabla v_1||_{0,K},\end{aligned}$$

where we used (14). Invoking this inequality in (22), we obtain

$$||w||_{0,K} \le \sqrt{2}\,(1 + C_4)\left(\frac{\kappa^{1/2} h_K^{1/2}}{a_1^{3/2}} + \frac{\kappa}{a_1^2}\right)||\boldsymbol{a} \cdot \nabla v_1||_{0,K}. \tag{23}$$

Next we bound $||\Phi||_{0,K}$. Observe that Φ is continuous on ∂K, so $\Phi \in C^2(\Omega) \cap C(\bar{\Omega})$. The operator L satisfies a maximum principle on K; see [18]. The smoothness of Φ means that we can construct a suitable barrier function for it. (Recall that a barrier function θ satisfies $|\Phi| \le \theta$ on ∂K, $|L\Phi| \le L\theta$ on K; these conditions imply that $|\Phi| \le \theta$ on all of K; see [18].) We shall do this for the case where ∂K^+ consists of two edges of K; the case where ∂K^+ is a single edge is similar but easier.

Let the two edges in ∂K^+ be E_1 and E_2, where the equation of E_i is $x = m_i' y + k_i'$ for $i = 1, 2$, and the m_i' and k_i' are constants. Extend each edge E_i to form a complete line (which we still call E_i). Given $(x, y) \in K$, define $x_i^+ = x_i^+(x, y)$ by the requirement that (x_i^+, y) lie on E_i. Set $M_1 = \max_{\partial K^+}\{|v_1(x^-) - v_1(x^+)|\}$ and $M_2 = 1 + (m_1')^2 + (m_2')^2$. Define the function $\theta_i(x, y)$ by

$$\theta_i(x, y) = M_1 e^{-a_1(x_i^+ - x)/(\kappa M_2)}, \quad \text{for } i = 1, 2.$$

For each i, a calculation shows that

$$L\theta_i(x, y) = \frac{a_i^2}{\kappa M_2}\left(1 - \frac{1 + (m_i')^2}{M_2}\right)\theta_i \ge 0,$$

by choice of M_2. Now set $\theta(x,y) = \theta_1(x,y) + \theta_2(x,y)$. Then $L\theta = L\theta_1 + L\theta_2 \geq 0 = L\Phi$ on K, and if $(x,y) \in \partial K^+$, then

$$\theta(x,y) = \theta_1(x,y) + \theta_2(x,y) > M_1 \geq \Phi(x,y),$$

for by construction $\theta_i = M_1$ on E_i; also $\theta > 0 = \Phi$ on ∂K^-. That is, we have shown that θ is a barrier function for Φ on K. The maximum principle now implies that $|\Phi| \leq \theta$ on K. Consequently

$$\begin{aligned}
||\Phi||_{0,K} &\leq ||\theta||_{0,K} \\
&\leq \left\{ \int_{(x^+,y)\in\partial K^+} \int_{(x^-,y)}^{(x^+,y)} 2\left(M_1^2 e^{-2a_1(x_1^+ - x)/(\kappa M_2)} + M_1^2 e^{-2a_1(x_2^+ - x)/(\kappa M_2)} \right) dx\, d\Gamma \right\}^{1/2} \\
&\leq M_1 \left\{ \int_{(x^+,y)\in\partial K^+} \frac{2\kappa M_2}{a_1}\, d\Gamma \right\}^{1/2} \\
&\leq \frac{2M_1\sqrt{M_2}\kappa^{1/2}h_K^{1/2}}{a_1^{1/2}} \\
&\leq \frac{2\sqrt{M_2}\kappa^{1/2}h_K^{3/2}|(\boldsymbol{a}\cdot\nabla v_1)_K|}{a_1^{3/2}} \\
&\leq \frac{2\sqrt{M_2}C_3\kappa^{1/2}h_K^{1/2}||\boldsymbol{a}\cdot\nabla v_1||_{0,K}}{a_1^{3/2}},
\end{aligned} \tag{24}$$

where, since $\boldsymbol{a}\cdot\nabla v_1$ is constant on each K, it follows from the regularity of the triangulation that $M_1 \leq h_K|(\boldsymbol{a}\cdot\nabla v_1)_K|/a_1$ and $h_K|(\boldsymbol{a}\cdot\nabla v_1)_K| \leq C_3||\boldsymbol{a}\cdot\nabla v_1||_{0,K}$ for some constant C_3.

By a triangle inequality,

$$||z||_{0,K} \leq ||w||_{0,K} + ||\Phi||_{0,K} \leq C_5 \left(\frac{\kappa^{1/2}h_K^{1/2}}{a_1^{3/2}} + \frac{\kappa}{a_1^2} \right) ||\boldsymbol{a}\cdot\nabla v_1||_{0,K},$$

from (23) and (24), where $C_5 = \sqrt{2}\,(1 + C_4) + 2\sqrt{M_2}\,C_3$. ■

Now we can finally obtain our coercivity result.

Theorem 1 *Assume that*

$$\kappa \leq h_K|\boldsymbol{a}| \min\left\{ 1, \frac{C_2^2}{64C_5^2} \right\} \tag{25}$$

for all triangles K in the triangulation. Then

$$a(\tilde{v}_h, v_1) \geq \sum_K \left(\kappa|v_1|_{1,K}^2 + \frac{C_2 h_K}{4|\boldsymbol{a}|} \int_K (\boldsymbol{a}\cdot\nabla v_1)^2\, ds \right),$$

where C_2 and C_5 were defined in Lemmas 2 and 3 respectively.

Proof: Lemma 3 shows that

$$|(\hat{v}_b^0 - v_b^0, \boldsymbol{a}\cdot\nabla v_1)_K| \le C_5 \left(\frac{\kappa^{1/2} h_K^{1/2}}{|\boldsymbol{a}|^{3/2}} + \frac{\kappa}{|\boldsymbol{a}|^2} \right) ||\boldsymbol{a}\cdot\nabla v_1||_{0,K}^2. \tag{26}$$

By (17), Lemma 2 and (26),

$$\begin{aligned} a(\tilde{v}_h, v_1) &= \sum_K \left(\kappa |v_1|_{1,K}^2 + \frac{1}{2|\boldsymbol{a}|^2} \int_{x^+\in\partial K^+} \left(\int_{x^-}^{x^+} \boldsymbol{a}\cdot\nabla v_1 \, ds \right)^2 \boldsymbol{a}\cdot\boldsymbol{n} \, d\Gamma \right) \\ &\qquad + \sum_K (\hat{v}_b^0 - v_b^0, \boldsymbol{a}\cdot\nabla v_1)_K \\ &\ge \sum_K \left(\kappa |v_1|_{1,K}^2 + \frac{C_2 h_K}{2|\boldsymbol{a}|} \int_K (\boldsymbol{a}\cdot\nabla v_1)^2 \, ds - C_5 \left(\frac{\kappa^{1/2} h_K^{1/2}}{|\boldsymbol{a}|^{3/2}} + \frac{\kappa}{|\boldsymbol{a}|^2} \right) ||\boldsymbol{a}\cdot\nabla v_1||_{0,K}^2 \right) \\ &\ge \sum_K \left(\kappa |v_1|_{1,K}^2 + \frac{C_2 h_K}{4|\boldsymbol{a}|} \int_K (\boldsymbol{a}\cdot\nabla v_1)^2 \, ds \right), \end{aligned}$$

where we used (25) for the last inequality (consider separately the cases $C_2^2 \le 64 C_5^2$ and $C_2^2 > 64 C_5^2$). ■

This is the desired coercivity inequality. The stability inequality derived in [4] is the limiting case ($\kappa = 0$) of Theorem 1. The large mesh-Peclet number hypothesis (25) is not a serious practical restriction; if it is violated for some K, then the mesh is locally fine relative to the diffusion parameter κ and the use of a stabilization technique (such as bubbles) is not crucial.

As a corollary, Lemma 2 then implies that in the piecewise linear case the RFB method is just as stable as the SDFEM/SUPG method.

Lemma 1 implies that our RFB method is, in general, less stable than the usual SDFEM/SUPG method that uses a piecewise polynomial trial space V_{h1}. Nevertheless this apparent loss of relative stability appears to be minor; see the numerical results in [4, 5].

We can see from the proof of Theorem 1 that coercivity is induced by the component $\tilde{v}_h = v_1 + v_b^0$ of v_h; the component v_b^f plays no part here. That is, *stability is induced by the L-spline component $\tilde{v}_h$ of the trial function v_h.* The remaining component v_b^f, which appears on the right-hand side of (12), affects only the consistency of the method. Thus our argument does not rely on the fact that the chosen bubble is residual-free; it will still be valid if v_b^f is replaced by any other choice that satisfies $v_b^f = 0$ on each ∂K and is independent of $\tilde{v}_h$.

4 A Two-Level Finite Element Method

To find the residual-free bubble part of the solution, u_b, we need to solve (5) that depends on the linear part of the solution, u_1. Instead, we can solve for the bubble shape functions

φ_i's and φ_f, with i varying from one to the number of element nodes (n_{en}):

$$L\varphi_i = -L\psi_i \qquad \text{in } K \tag{27}$$
$$\varphi_i = 0 \qquad \text{on } K\,. \tag{28}$$

where the ψ_i's are the local basis functions for u_1 and

$$L\varphi_f = f \qquad \text{in } K \tag{29}$$
$$\varphi_f = 0 \qquad \text{on } K\,. \tag{30}$$

Thus, if

$$u_1 = \sum_i c_i \psi_i\,,$$

then

$$u_b = \sum_i c_i \varphi_i + \varphi_f\,,$$

and substituting into (7) we get the matrix formulation

$$\sum_i c_i [a(\psi_i, \psi_j) + a(\varphi_i, \psi_j)] = (f, \psi_j) - a(\varphi_f, \psi_j). \tag{31}$$

It turns out that the first step of this procedure may be as complex as trying to solve the original PDE problem. Therefore, we consider the following strategy. At the pre-processing stage of a finite element code, consider approximating the differential equations for the bubble shape functions φ_i's and φ_f, (equations (27)-(30)) by another finite element method. In other words, for each element we consider a sub-mesh (a mesh defined for each element) where we will solve the equations (27)-(30)) by a suitable finite element method. This can be done using a non-standard method: the Galerkin-least squares method (GLS), for example. We will need to repeat this procedure for each element and for each basis function.

Let us now describe the application of this strategy to the advection-diffusion problem using the GLS method to solve each bubble problem. We have in this case a two-level finite element method. At the global level we are using the Galerkin method with piecewise linears for the original method, and at each element level we discretize again and solve the bubble problems using GLS. Thus corresponding to (27)-(30) we need to solve in each element K of the original mesh:

$$\begin{aligned} \boldsymbol{a}\cdot\nabla\varphi_i - \kappa\triangle\varphi_i &= -\boldsymbol{a}\cdot\nabla\psi_i \qquad i = 1, .., n_{en} \qquad \text{in } K \\ \varphi_i &= 0 \quad \text{on } \partial K \end{aligned}$$

To construct the GLS approximation of this differential problem, let us denote by K^* an arbitrary element in the submesh with diameter h^* and by ψ_l^* the basis function for a

piecewise linear interpolation in the submesh, so that our unknown bubble basis function φ_i can be approximated by

$$\varphi_i^{h^*} = \sum_l c_l^{(i)} \psi_l^* \tag{32}$$

Here l runs over all unknown interior nodes in the submesh, say through N^*. The index i refers to the specific bubble function that we are trying to compute. (Recall that we need to solve for a number of bubbles equals to the number of basis functions used to span the piecewise polynomial defined in the global element K.)

We then formulate the GLS method in matrix formulation as: for each i (from 1 to n_{en}) find $c_l^{(i)}$, $l = 1, 2, .., N^*$ such that

$$\sum_l c_l^{(i)} [(\boldsymbol{a} \cdot \nabla \psi_l^*, \psi_m^*) + (\kappa \nabla \psi_l^*, \nabla \psi_m^*) + (\boldsymbol{a} \cdot \nabla \psi_l^*, \tau \boldsymbol{a} \cdot \nabla \psi_m^*)] = (-\boldsymbol{a} \cdot \nabla \psi_{i,K}, \psi_m^* + \tau \boldsymbol{a} \cdot \nabla \psi_m^*) \tag{33}$$

for $m = 1, 2, .., N^*$. We use the stability parameter τ given in [7] as:

$$\tau(x, Pe_K(x)) = \frac{h_K}{2|\boldsymbol{a}|_2} \xi(Pe_K(x)), \tag{34}$$

$$Pe_K(x) = \frac{|\boldsymbol{a}(x)|_2 h_K}{6\kappa(x)}, \tag{35}$$

$$\xi(Pe_K(x)) = \begin{cases} Pe_K(x), & \text{if } 0 \le Pe_K(x) < 1, \\ 1.0, & \text{if } Pe_K(x) \ge 1, \end{cases} \tag{36}$$

$$|\boldsymbol{a}(x)|_2 = \left(\sum_{i=1}^{2} |a_i(x)|^2 \right)^{1/2}, \tag{37}$$

Once the constants $c_l^{(i)}$'s are found, we substitute them in (32) to get the approximate residual basis function $\varphi_i^{h^*}$. These approximations are then assembled to the global problem

$$\sum_{i=1} c_i [(\boldsymbol{a} \cdot \nabla \psi_i, \psi_j) + (\kappa \nabla \psi_i, \nabla \psi_j) + (\boldsymbol{a} \cdot \nabla \varphi_i, \psi_j)] = (f, \psi_j) - (\boldsymbol{a} \cdot \nabla \varphi_f, \psi_j) \tag{38}$$

in place of the exact residual function φ_i. The global problem may now be solved for the piecewise-linear part of the solution. We then recover the bubble part of the solution by

$$u_b = \sum_i c_i \varphi_i + \varphi_f, \tag{39}$$

with $\varphi_i^{h^*}$ in lieu of φ_i.

5 Some Numerical Results

In this section we report three series of experiments for convection-diffusion problems with the two-level finite element introduced in the previous section. We compare our results with those obtained by the GLS method used in the entire domain.

5.1 Advection in a rotating flow field

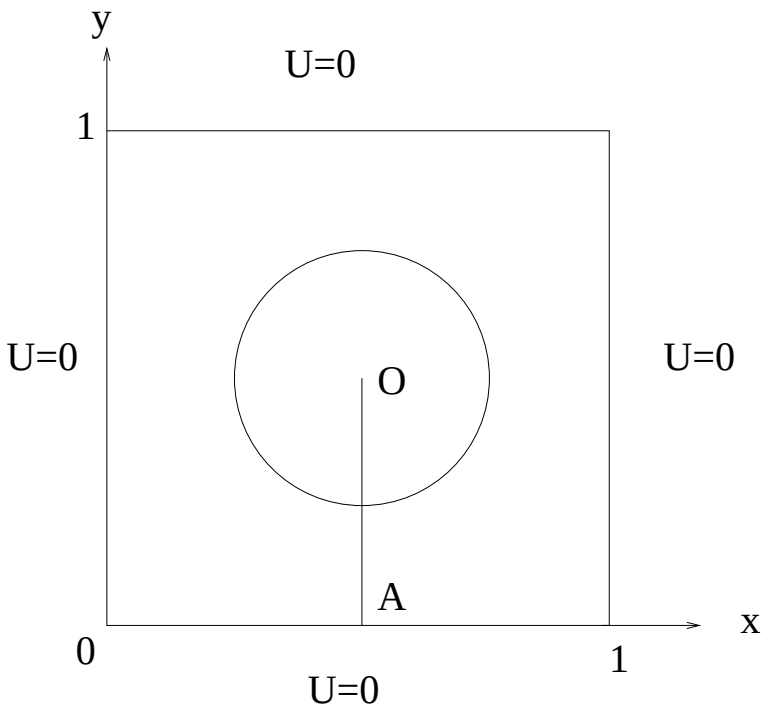

Figure 1: Statement of rotating flow field problem

This problem is defined on a unit square of coordinates $0 \leq x, y \leq 1$, where the flow velocity components are given by

$$a_1 = -(y - 0.5), \qquad a_2 = x - 0.5$$

Along the external boundary $u = 0$ and along the internal boundary (OA),

$$u = \frac{1}{2}(\cos(4\pi y - \pi) + 1), \qquad 0 \leq y \leq 0.5$$

(see Fig.1 for problem statement). The diffusivity is $\kappa = 10^{-6}$. A uniform mesh with 30x30 elements is employed with bilinear elements $Q1$. Two-level results are obtained by subdividing each element into 7x7 subelements: each subelement is generated by a linear mapping from a uniform subdivision with 7x7 subelements in the reference square

domain. In plotting the following results, we have not added the bubble part of the solution to the bilinear part in the two-level method.

Elevation plots are shown in Fig.2 for GLS and TLFEM methods. In this problem, both methods perform well and the results are almost indistinguishable.

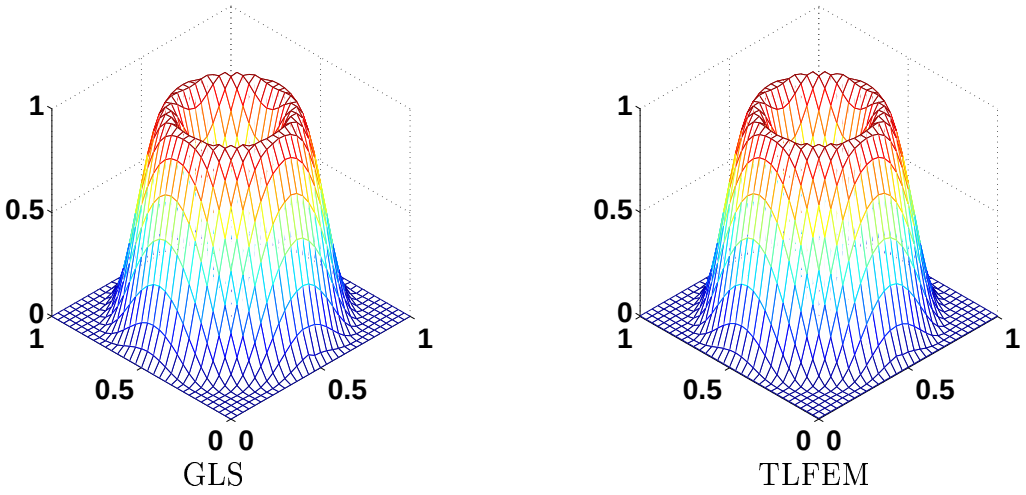

Figure 2: Advection in a rotating flow field: Elevation plots for GLS versus TLFEM

5.2 Thermal Boundary Layer Problem

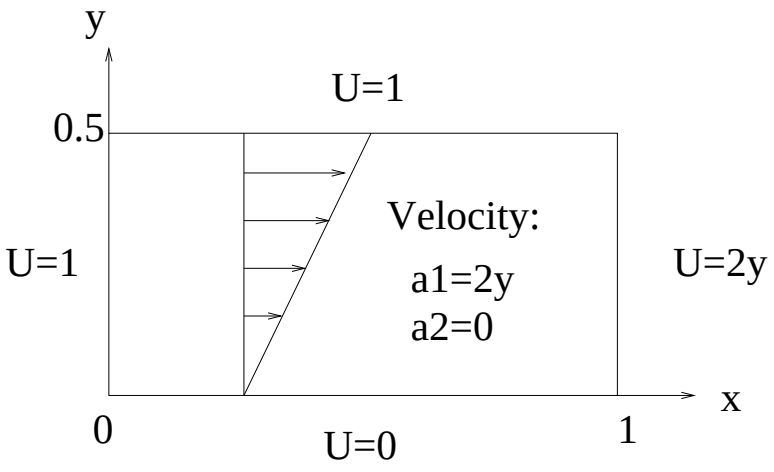

Figure 3: Statement of thermal boundary layer problem

Let us consider a rectangular domain of sides 1.0 and 0.5, subjected to the following boundary conditions (see Fig.3 for problem statement):

$$u = 1, \qquad \text{when} \begin{cases} x = 0, & \text{if } 0 \leq y \leq 0.5, \\ y = 0.5, & \text{if } 0 \leq x \leq 1.0, \end{cases} \tag{40}$$

$$u = 0, \qquad \text{when } y = 0,\ 0 < x \leq 1.0,$$

$$u = 2y, \qquad \text{when } x = 1,\ 0 < y < 0.5.$$

The flow components are

$$a_1 = 2y, \qquad a_2 = 0 \qquad \text{in } \Omega$$

and the diffusivity is $\kappa = 7\text{x}10^{-4}$. This problem may be viewed as the simulation of the development of a thermal boundary layer on a fully developed flow between two parallel plates, where the top plate is moving with velocity equal to one and the bottom plate is fixed. Taking the top plate velocity as the characteristic flow velocity, we have for this flow a Peclet number $Pe = 714$.

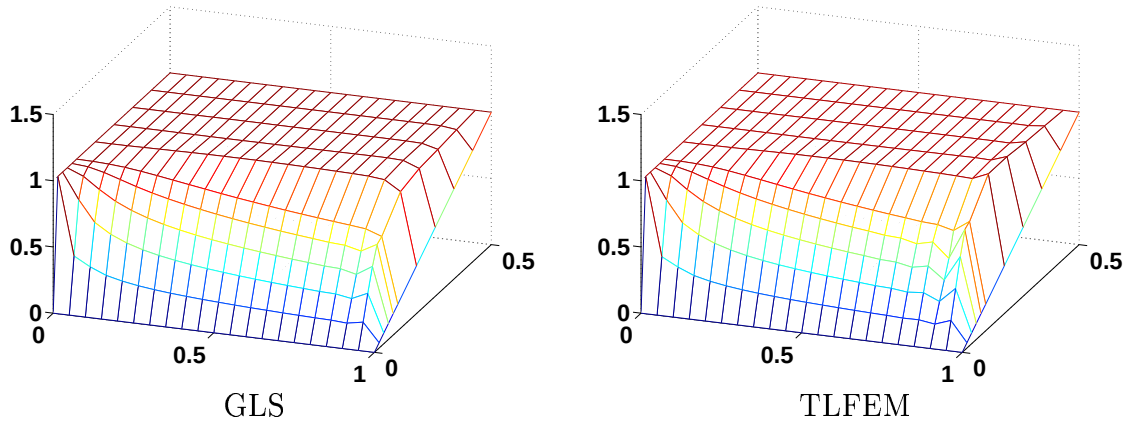

Figure 4: Thermal boundary layer problem: Elevation plots for GLS versus TLFEM

We employ a rectangular mesh consisting of 21 equally spaced nodes in the x-direction, 6 nodes uniformly distributed in the interval $0 \leq y \leq 0.1$ and 6 nodes equally spaced on $0.1 \leq y \leq 0.5$. We also subdivide each element into 20x20 subelements: each subelement is generated by a bilinear mapping from a uniform subdivision with 20x20 subelements in the reference square domain.

In this problem, both GLS and TLFEM perform similarly except in the neigborhood of the outflow boundary layer (see Fig.4). TLFEM is a little more accurate than GLS therein.

5.3 An example with analytical solution

In the convergence analysis, we consider a simple problem on a unit square that can be solved analytically, so that we can compare the GLS and TLFEM results with the exact solution. Consider the unit square subjected to the following boundary conditions (see Fig.5 for problem statement) :

$$u = 0 \qquad \text{when } \begin{cases} x = 0, & \text{if } 0 \leq y \leq 1.0, \\ y = 1.0, & \text{if } 0 \leq x \leq 1.0, \\ x = 1, & \text{if } 0 \leq y \leq 1.0, \end{cases} \tag{41}$$

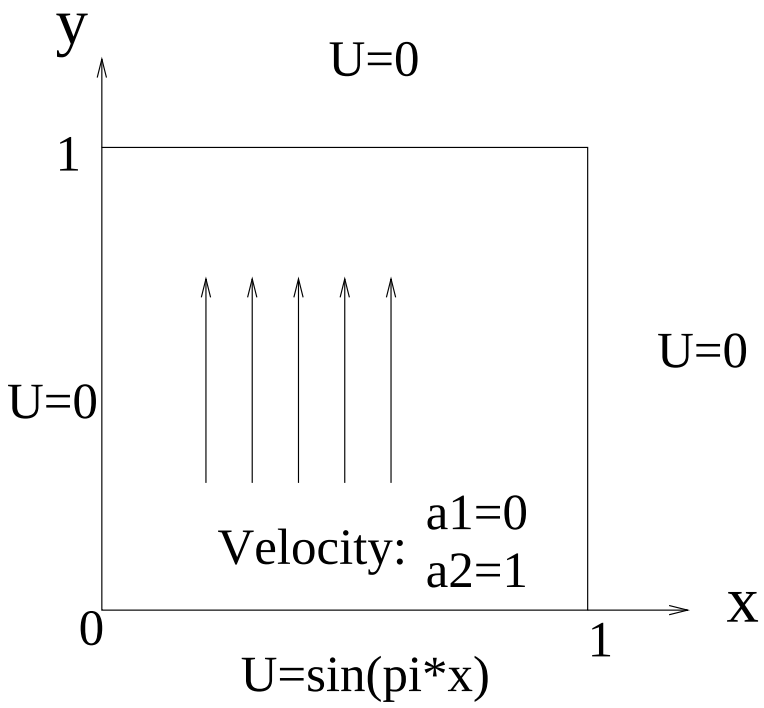

Figure 5: Problem statement of an example with analytical solution

$$u = \sin(\pi x), \qquad y = 0, \qquad 0 < x \leq 1.0;$$

The flow components are

$$a_1 = 0, \qquad a_2 = 1.0 \qquad \text{in } \Omega\,.$$

Using separation of variables, the exact solution is given by :

$$u = \frac{1}{e^{m_2 - m_1} - 1}(e^{m_2 - m_1} e^{m_1 y} - e^{m_2 y}) \sin(\pi x)$$

where

$$m_1 = \frac{1 - \sqrt{1 + 4\kappa^2\pi^2}}{2\kappa}$$

and

$$m_2 = \frac{1 + \sqrt{1 + 4\kappa^2\pi^2}}{2\kappa}\,.$$

We consider two different values for the diffusivity, namely, $\kappa = 0.01$ and $\kappa = 1.0$. We compute the L_2 and H_1 errors using 25-point Gaussian quadrature on each global element except for the rows of elements between $0.9 \leq y \leq 1$, where there is an outflow boundary layer for $\kappa = 0.01$. The TLFEM approximation is obtained by subdividing each global element into 5x5 subelements. The results are shown in Figs. 6-9. We obtain second order convergence in the L_2 norm and first order in the H_1 norm when $\kappa = 1$, but for $\kappa = 0.01$, the convergence rate slightly decreases for both and the GLS method is slightly more accurate than TLFEM.

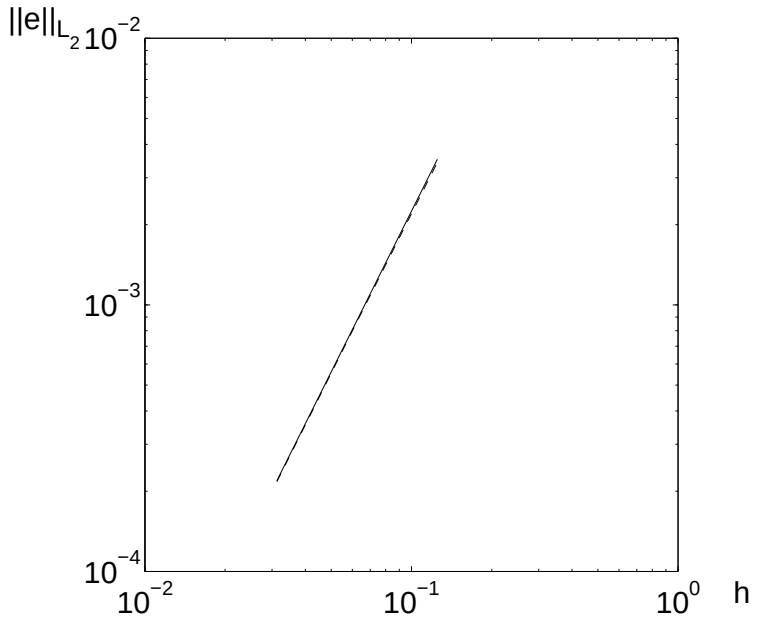

Figure 6: Comparison of L_2 errors for $\kappa = 1$: TLFEM (thick) and GLS (dashed)

6 Conclusions

We considered the application of residual-free bubble functions to convection-diffusion problems in two dimensions when the underlying polynomial space consists of piecewise linears. We showed that the method is as stable as the streamline diffusion method for large mesh Peclet numbers. Furthermore, our analysis reveals that this stability is due to the L-spline component of the bubble; the rest of the bubble affects only the consistency/accuracy of the method. These results are obtained under the hypotheses that the flow velocity field is constant, the triangulation is regular (and this regularity is uniform as the mesh diameter tends to zero), and all edges of the triangulation are bounded away from the direction of the flow. The restriction of the results to lage mesh Peclet numbers is probably an artifact of the arguments that we used; of course when the mesh Peclet number is not large, many numerical methods are suitable for these problems.

An application of the two-level finite element method introduced in [8] for the Helmholtz equation is also studied herein for the advection-diffusion equation. The method approximates the computation of the residual-free bubble basis functions by a stabilized method (GLS) and uses these approximations to compute the bilinear part of the solution using the Galerkin method. Approximation in a nonstandard fashion is confined to the computations of the bubbles, with the driving method being the Galerkin method, without any numerical tricks. The numerical results confirm good accuracy and stability properties of the Galerkin method enriched with (approximate) residual-free bubbles. Careful cost effectiveness studies of this approach versus standard stabilized methods (GLS, for example) need to be addressed.

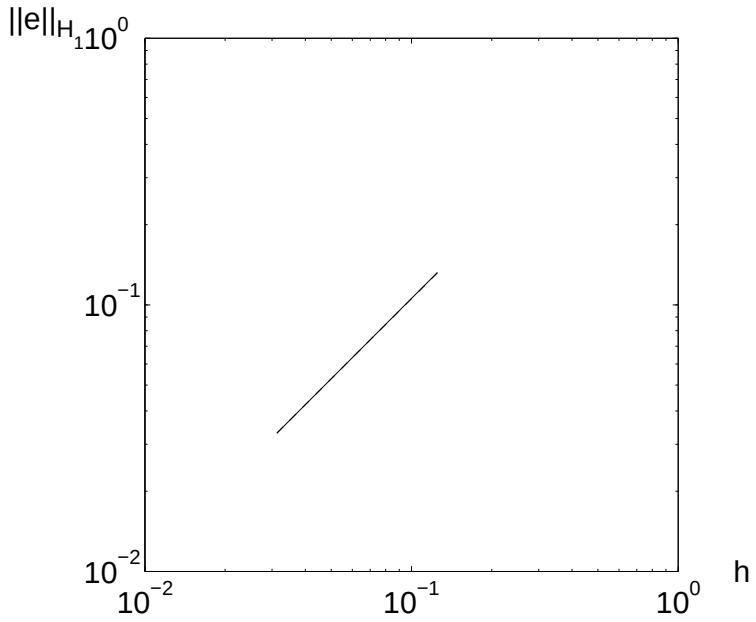

Figure 7: Comparison of H_1 errors for $\kappa = 1$: TLFEM (thick) and GLS (dashed)

7 Acknowledgment

During the course of this work Martin Stynes was on sabbatical leave at the University of Colorado at Denver, and he gratefullly acknowledges support from University College Cork and NSF grant DMS-9312752 under the direction of Prof. Tom Russell.

References

[1] C. Baiocchi, F. Brezzi, and L.P. Franca. Virtual bubbles and the Galerkin-least-squares method. *Comput. Methods Appl. Mech. Engrg.*, 105:125–141, 1993.

[2] F. Brezzi, M.O. Bristeau, L.P. Franca, M. Mallet, and G. Rogé. A relationship between stabilized finite element methods and the Galerkin method with bubble functions. *Comput. Methods Appl. Mech. Engrg.*, 96:117–129, 1992.

[3] F. Brezzi, L. P. Franca, T. J. R. Hughes, and A. Russo. $b = \int g$. *Comput. Methods Appl. Mech. Engrg.*, 145:329–339, 1997.

[4] F. Brezzi, L. P. Franca, and A. Russo. Further considerations on residual-free bubbles for advective-diffusive equations. To appear.

[5] F. Brezzi and A. Russo. Choosing bubbles for advection-diffusion problems. *Math. Models Meth. Appl. Sci.*, 4:571–587, 1994.

[6] L. P. Franca and C. Farhat. Bubble functions prompt unusual stabilized finite element methods. *Comput. Methods Appl. Mech. Engrg.*, 123:299–308, 1995.

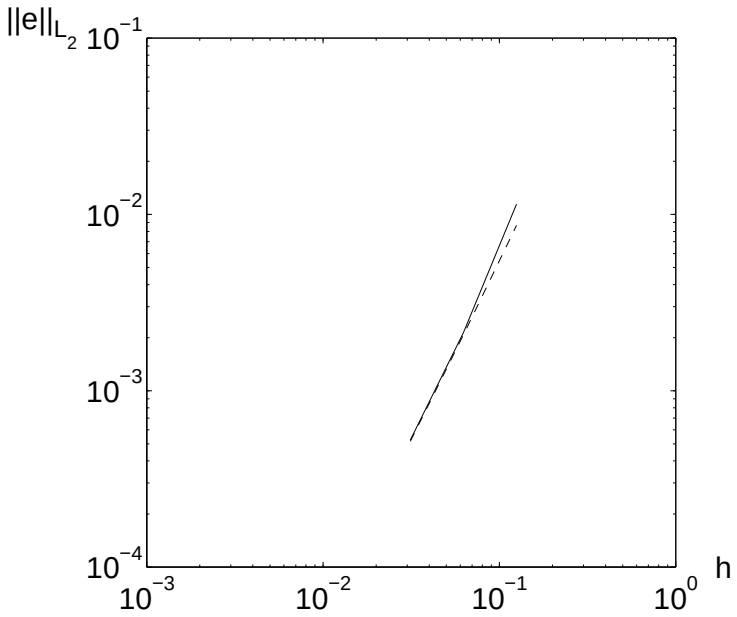

Figure 8: Comparison of L_2 errors for $\kappa = 0.01$: TLFEM (thick) and GLS (dashed)

[7] L. P. Franca, S. L. Frey, and T. J. R. Hughes. Stabilized finite element methods: I. Application to the advective-diffusive model. *Comput. Methods Appl. Mech. Engrg.*, 95:253–276, 1992.

[8] L. P. Franca and A. P. Macedo. A two-level finite element method and its application to the Helmholtz equation. To appear.

[9] L. P. Franca and A. Russo. Approximation of the Stokes problem by residual-free macro bubbles. *East-West J. Appl. Math.*, 4:265–278, 1996.

[10] L. P. Franca and A. Russo. Deriving upwinding, mass lumping and selective reduced integration by residual-free bubbles. *Appl. Math. Letters*, 9:83–88, 1996.

[11] L. P. Franca and A. Russo. Mass lumping emanating from residual-free bubbles. *Comput. Methods Appl. Mech. Engrg.*, pages 353–360, 1997.

[12] L. P. Franca and A. Russo. Unlocking with residual-free bubbles. *Comput. Methods Appl. Mech. Engrg.*, pages 361–364, 1997.

[13] A. F. Hegarty, E. O'Riordan, and M. Stynes. A comparison of uniformly convergent difference schemes for two-dimensional convection-diffusion problems. *J. Comput. Phys.*, 105:24–32, 1993.

[14] T. J. R. Hughes. Multiscale phenomena: Green's functions, the Dirichlet-to-Neumann formulation, subgrid scale models, bubbles and the origin of stabilized methods. *Comput. Methods Appl. Mech. Engrg.*, 127:387–401, 1995.

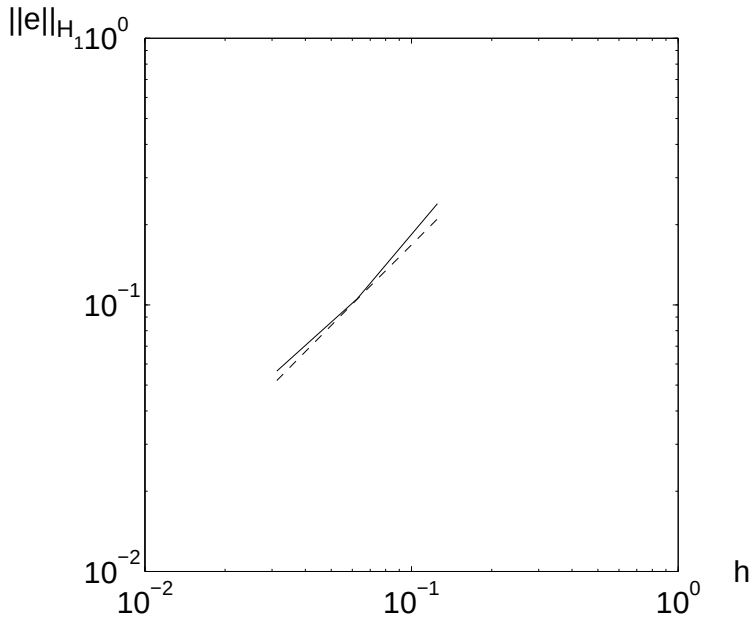

Figure 9: Comparison of H_1 errors for $\kappa = 0.01$: TLFEM (thick) and GLS (dashed)

[15] T. J. R. Hughes, L. P. Franca, and G. M. Hulbert. A new finite element formulation for computational fluid dynamics: VIII. The Galerkin-least-squares method for advective-diffusive equations. *Comput. Methods Appl. Mech. Engrg.*, 73:173–189, 1989.

[16] C. Johnson, U. Nävert, and J. Pitkäranta. Finite element methods for linear hyperbolic problem. *Comput. Methods Appl. Mech. Engrg.*, 45:285–312, 1984.

[17] E. O'Riordan and M. Stynes. A globally uniformly convergent finite element method for a singularly perturbed elliptic problem in two dimensions. *Math. Comp.*, 57:47–62, 1991.

[18] M. H. Protter and H. F. Weinberger. *Maximum Principles in Differential Equations.* Prentice-Hall, New Jersey, 1967.

[19] H.-G. Roos, M. Stynes, and L. Tobiska. *Numerical Methods for Singularly Perturbed Differential Equations.* Springer Verlag, Berlin, 1996.

[20] R. Sacco and M. Stynes. Finite element methods for convection-diffusion problems using exponential splines on triangles. *Computers Math. Applic.*, 35:35–45, 1998.